韓國鑛物學會誌 第2券 第2號
J.Miner.Soc. Korea, 2, 81－89(1989)

Mineralogy of Alunite from the Sungsan Mine

聲山鑛山 明礬石의 鑛物學的 特性

Hyen Goo Cho(曺 鉉 丘) and Soo Jin Kim(金 洙 鎭)

Department of Geological Sciences, Seoul National University, Seoul 151-742, Korea
서울大學校 自然科學大學 地質科學科

ABSTRACT: Alunite occurs as massive, cavity-filling and veinlets in the Cretaceous Hwangsan Formation in the Sungsan mine, Korea. It is a hydrothermal alteration product of rhyolitic tuffs, and associated with dickite, quartz and barite.

The average chemical formula of alunite in the mine is $(K_{0.93}Na_{0.07})_{1.00}Al_{3.00}(SO_4)_{2.00}(OH)_6$. Atomic percentage of Na substituting for K in A site of the alunite structure varies from 5.9 to 9.2. Unit-cell volume and c dimension decrease with increasing Na atomic percentage.

On the basis of thermal and high temperature XRD analyses, the decomposition of alunite into $KAl(SO_4)_2$ and $NaAl(SO_4)_2$ concomitant with the liberation of structural water (12.86%) occurs at about 550°C. The reconstruction of $KAl(SO_4)_2$ and $NaAl(SO_4)_2$ to $Al_2(SO_4)_3$, arcanite and thenardite, and the crystallization of γ-Al_2O_3 take place at about 720°C. The destruction of $Al_2(SO_4)_3$ structure takes place at about 760°C removing 3/4 of total SO_3 (27.32%).

要約 : 聲山鑛山의 明礬石은 白堊紀 黃山凝灰岩層에서 3가지 형태, 즉 塊狀, 空洞充塡狀 및 細脈狀으로 산출된다. 明礬石은 流紋岩質擬灰岩이 熱水變質作用을 받아 형성된 것으로 생각되며, 딕카이트, 石英과 重晶石을 隨伴한다.

EPMA分析을 통하여 구해진 聲山鑛山 明礬石의 평균화학조성은 $(K_{0.93}\ Na_{0.07})Al_{3.00}(SO_4)_{2.00}(OH)_6$로써, 明礬石 構造의 A자리에 K를 置換하는 Na의 原子含量은 5.9에서 9.2%까지 변화한다. Na의 原子含量이 증가할수록 單位胞의 부피와 c축은 감소한다.

明礬石의 熱分析 및 高溫 X線回折分析에 의하면, 構造水의離脫(12.86%)을 수반하는 明礬石구조의 破壞는 약 550℃에서 일어나고, 無水明礬의 $Al_x(SO_4)_3$, arcanite와 thenardite로의 轉移 및 γ-Al_2O_3의 結晶化는 약 720℃에서 일어난다. 또한 전체 SO_3의 3／4의 烝氣化 (27.32%)를 수반하는 $Al_2(SO_4)_3$의 파괴는 약 760℃에서 일어난다.

INTRODUCTION

The Sungsan mine where the alunite occurs as the hydrothermal alteration product of volcanic rocks, is located 27 km south of Mokpo City and 25 km west of Haenam, Jeonranam-do, Korea. The mine produces monthly about 5,000 tons of "napseok" (aglamatolite) and porcelain clay. Napseok is mainly composed of dickite, and porcelain clay consists of micro-crystalline quartz and dickite. Napseok and porcelain clay are commercial terms. Alunite is chiefly associated with napseok.

Alunite group minerals show a wide range in ionic substitution. They have general chemical formula, $AR_3(SO_4)_2(OH)_6$, in which A refers to K^+, Na^+, Pb^{2+}, NH_4^+ Ag^+, Sr^{2+}, Ca^{2+} or H_3O^+, and R refers to Fe^{3+} or Al^{3+}. In some cases, SO_4^{2-} may be replaced by PO_4^{3-} (Hendricks, 1937; Parker, 1962; Kubisz, 1970; Ossaka *et al.*, 1982; Ripmeester *et al.*, 1986; Stephen *et al.*, 1988).

Alunite group minerals have the space group $R\bar{3}m$ (or R3m). They can be described in terms of the hexagonal cell in which the a and c parameters are approximately 7 Å and 17 Å, re-

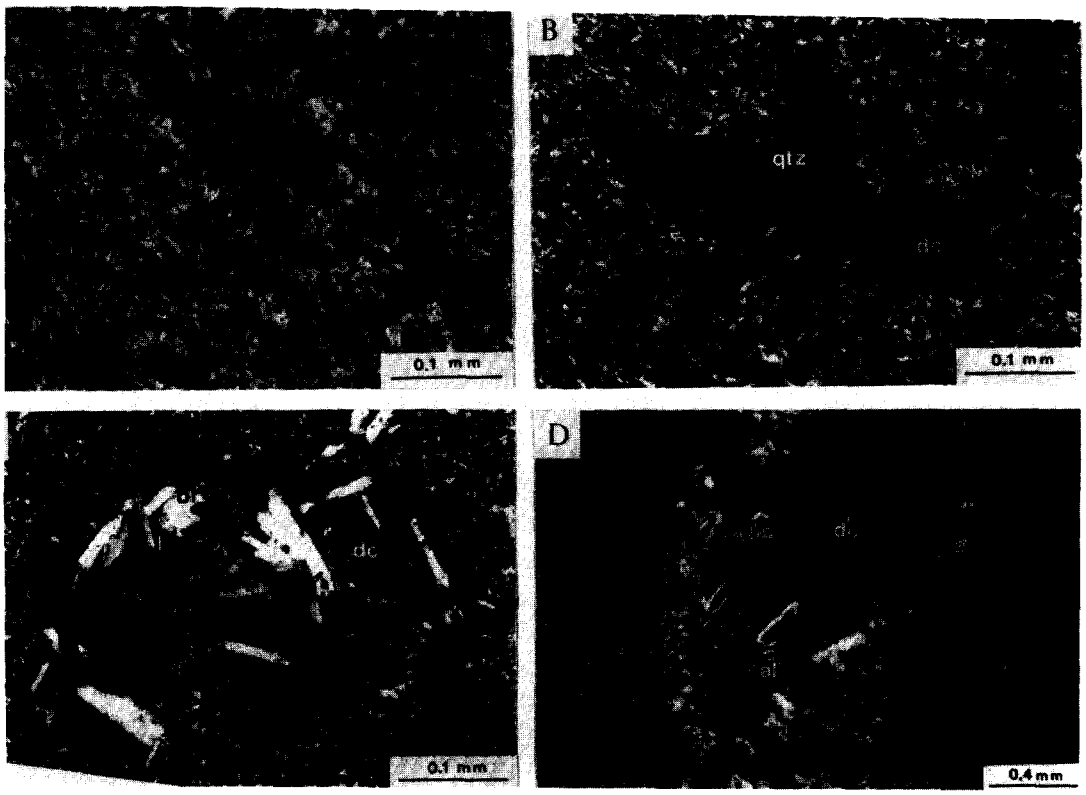

Fig. 1. Photomicrographs of alunite from the Sungsan mine (Crossed nicols): (A) Massive alunite consisting of fine-grained anhedral particles; (B) Massive alunite consisting of fine-grained prismatic grains in association with quartz (qtz) and dickite (dc); (C) Alunite (al) filling the cavity (cv) within the massive dickite (dc) mass. Barite (br) is associated with alunite; (D) Alunite-dickite veinlet in massive claystone. Note the zonal arrangement of alunite (al) and dickite (dc).

spectively (Hendricks, 1937; Parker, 1962; Wang *et al.*, 1965; Goreaud and Raveau, 1980). Sulfur ions are surrounded by four oxygens which form tetrahedra. R ions have 6-fold octahedral coordination surrounded by octahedra of 4 OH^- and 2 oxygens of SO_4^{2-} groups. Alkali ions occupy the A site in 12-fold coordination between the sheets of R octahedra.

Alunite-natroalunite series form a solid solution having the general chemical formula (K, Na)$Al_3(SO_4)_2(OH)_6$. By definition, alunite represents the member with the composition K > Na, whereas natroalunite refers to the member Na > K. Substitution between Na^+ and K^+ ions is isomorphous, and alkali ions may be substituted by H_3O^+ (Parker, 1962; Kubisz, 1970; Wilkins and Mateen, 1974; Ripmeester *et al.*, 1986), NH^{4+} (Hendricks, 1937; Stephen *et al.*, 1988), Ca^{2+} (Ossaka *et al.*, 1982; Scott, 1987), or other cations.

Crystal chemical studies of the natural and synthetic alunite group minerals (Brophy *et al.*, 1962; Parker, 1962; Menchetti and Sabelli, 1976; Ossaka *et al.*, 1982; Chitale and Güven, 1987; Stephen *et al.*, 1988), show that the c dimension is highly sensitive to substitution in alkali position, whereas the a dimension is affected by octahedral (Al, Fe) substitution.

This paper describes the occurrence, chemistry, structure, thermal and infrared properties of alunite from the Sungsan mine.

EXPERIMENTAL DETAILS

Textures of alunite were examined under the polarizing microscope and scanning electron

microscope (SEM). Nearly pure alunite samples were separated from alunite-rich specimens under the stereomicroscope for various works.

Mineral compositions of the various rocks and ores were determined by X-ray powder diffraction (XRD) analysis using a Rigaku model RAD 3-C and Ni-filtered CuKα radiation. X-ray diffraction data were indexed after Parker (1962). Refinement and calculation of the unit-cell demensions were done using the least squares program by the Appleman-Evans called LSUCRIPC (Appleman and Evans, 1973; Garvey, 1986).

Chemical composition and elemental distribution of alunite were analyzed using both the ernergy dispersive X-ray (EDX) and the wavelength dispersive X-ray (WDX) spectrometers. The SEM, EDX and WDX analyses were conducted with a JEOL electron probe microanalyzer model JXA-733 and LINK AN 10000. More than 350 counts were averaged for analyses of 5 polished-thin sections. H_2O was determined by thermogravimetric (TG) analysis.

Differential thermal analysis (DTA), TG analysis, and differential thermogravimetric (DTG) analysis were performed simultaneously using Rigaku model TSS Thermoflex. Sample about 50 mg was heated in air from room temperature (ca. 25°C) to 900°C at a rate of 10°C per minute, and α-Al_2O_3 was used as

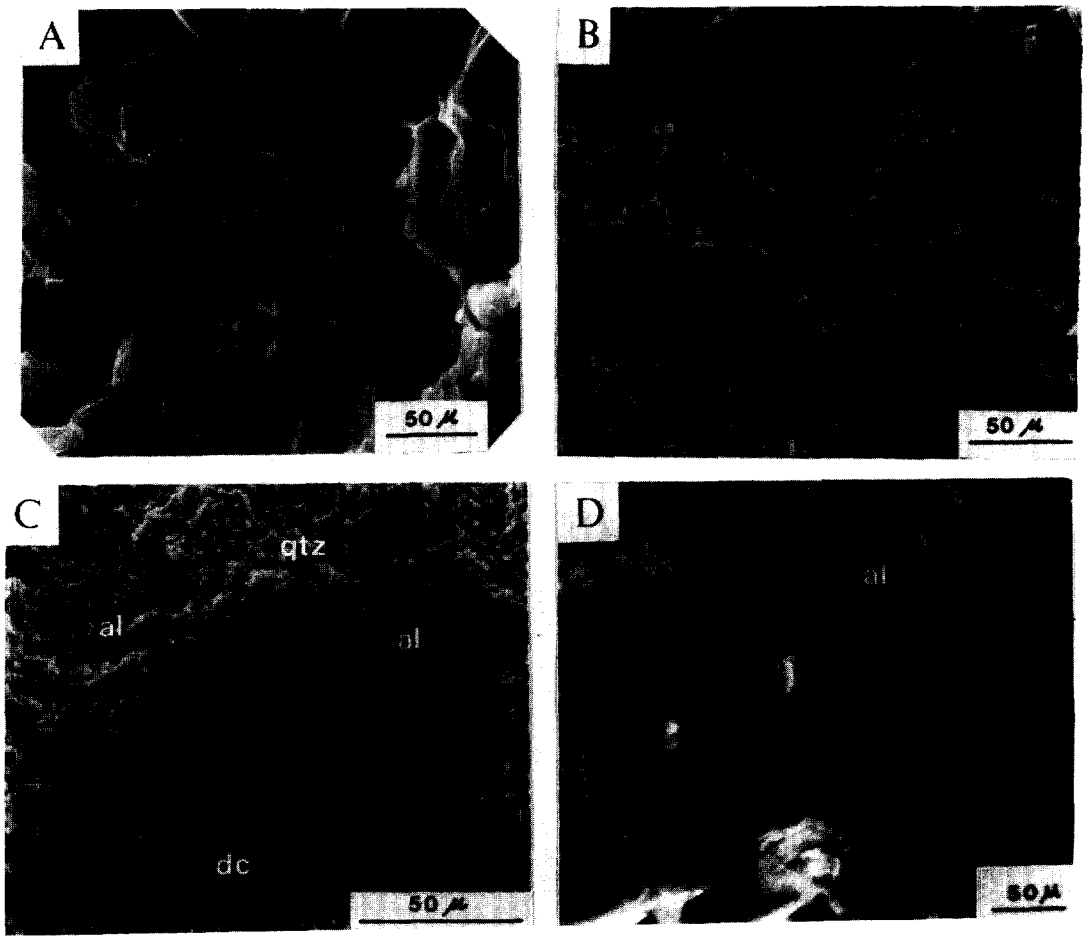

Fig. 2. SEM photographs of alunite from the Sungsan mine: (A) Massive alunite, (B) Short prismatic or tabular alunite in massive ore; (C) Long prismatic or tabular alunite (al) and dickite (dc) fill the cavity in the microcrystalline quartz (qtz) aggregates; (D) Rhombohedral alunite crystals (al) in veinlet.

standard material. Heating of the sample from 25°C to 1000°C was conducted using the High Temperature X-ray Diffractometer Attachment model CN2311B1 at a rate of 10°C per minute. At each temperature step of 100°C, samples were heated for 1 hour.

Infrared (IR) absorption spectra were recorded with a Perkin-Elmer model 283B Spectrophotometer. KBr pellet method was used over the range of 4,000 to 200 cm^{-1} under conditions of scan time 6 minutes, slit program 6 and expansion 1. Each spectrum was calibrated with polystyrene film. A standard pellet of KBr placed in the reference beam compensated for energy loss caused by KBr in the sample pellet.

OCCURRENCES

The Sungsan napseok deposit has been formed by hydrothermal alteration of the Cretaceous Hwangsan Tuff Formation consists of white to gray, fine to coarse vitric tuffs and lapillistones.

Alunite occurs as three different modes, that is, 1) massive, 2) cavity-filling and 3) veinlets (Figs. 1 and 2).

Massive alunite consists of anhedral, short prismatic or tabular crystals of 20 to 50 μm in length. In some cases, alunite replaces quartz or dickite (Figs. 1B and C).

Cavity-filling alunite is long prismatic or tabular in habit and 50 to 100 μm in length. It is associated with dickite and barite (Figs. 1A and 2A).

In alunite-dickite veinlets, alunite grows along the walls of veinlets whereas dickites is concentrated walls of veinlets whereas dickites is concentrated in the central part (Fig. 1D). Alunite shows rhombohedral crystals of 0.2 to 2 mm in size (Fig. 2D). The alunite-dickite veinlets are the final products of mineralization.

CHEMICAL COMPOSITIONS AND UNIT-CELL DIMENSIONS

Average compositions and structural formulae of alunite based on 11 oxygens are given in Table 1. Chemical formula calculated from the average composition of alunite from the Sungsan mine is $(K_{0.93}Na_{0.07})_{1.00}\ Al_{3.00}\ (SO_4)_{2.00}\ (OH)_6$. Atomic percentage of Na replacing K vary from 5.9 to 9.2, and substitution of Fe for Al and of P for S are negligible. Atomic percentage of Na substituting for K is lower in the prismatic alunite from cavity-filling or massive ores (C1, C3 and F4) than those from massive (A7) or veinlet alunites (A8).

Elemental distribution of alunite was analyzed by electron microprobe X-ray images for several large alunite grains from veinlet. Quantitative analyses were run at an interval of 15 μm along a

Table 1. Electron microprobe analyses and structural formulae of alunite from the Sungsan mine.

#	C1 (21)	C3 (22)	F4 (27)	A8 (260)	A7 (29)	average (359)
SiO_2	–**	0.19	–	0.02	0.06	0.09
TiO_2	–	0.09	–	0.07	0.06	0.07
Al_2O_3	36.96	37.02	36.84	36.88	36.60	36.90
Fe_2O_3*	0.06	0.08	0.04	0.09	0.09	0.07
K_2O	10.64	10.82	10.22	10.08	10.66	10.56
Na_2O	0.44	0.48	0.48	0.63	0.71	0.54
SO_3	38.26	38.78	38.18	38.76	38.64	38.55
P_2O_5	–	0.14	–	0.10	0.11	0.11
H_2O	–	–	–	–	12.86***	–
Total	86.35	87.61	85.76	86.63	99.80	86.89
Numbers of ions on the basis of 11 oxygens						
Al	3.018	2.990	3.020	2.992	2.974	2.998
Fe	0.003	0.004	0.002	0.005	0.005	0.003
$\Sigma 1$	3.021	2.994	3.022	2.997	2.979	3.001
K	0.941	0.946	0.908	0.885	0.937	0.929
Na	0.058	0.064	0.064	0.084	0.095	0.072
$\Sigma 2$	0.999	1.010	0.972	0.969	1.032	1.001
S	1.989	1.995	1.993	2.002	2.000	1.994
P	–	0.008	–	0.006	0.006	0.006
$\Sigma 3$	1.989	2.003	1.993	2.008	2.006	2.000
$Na/\Sigma 1$(%)	5.9	6.4	6.6	8.7	9.2	7.2
$Fe/\Sigma 2$(%)	0.1	0.1	0.1	0.2	0.2	0.1
$P/\Sigma 3$(%)	–	0.4	–	0.3	0.3	0.3

* Total Fe, ** Not analyzed, *** Determined by TG analysis.
Numbers in the parenthesis indicate total points for average.

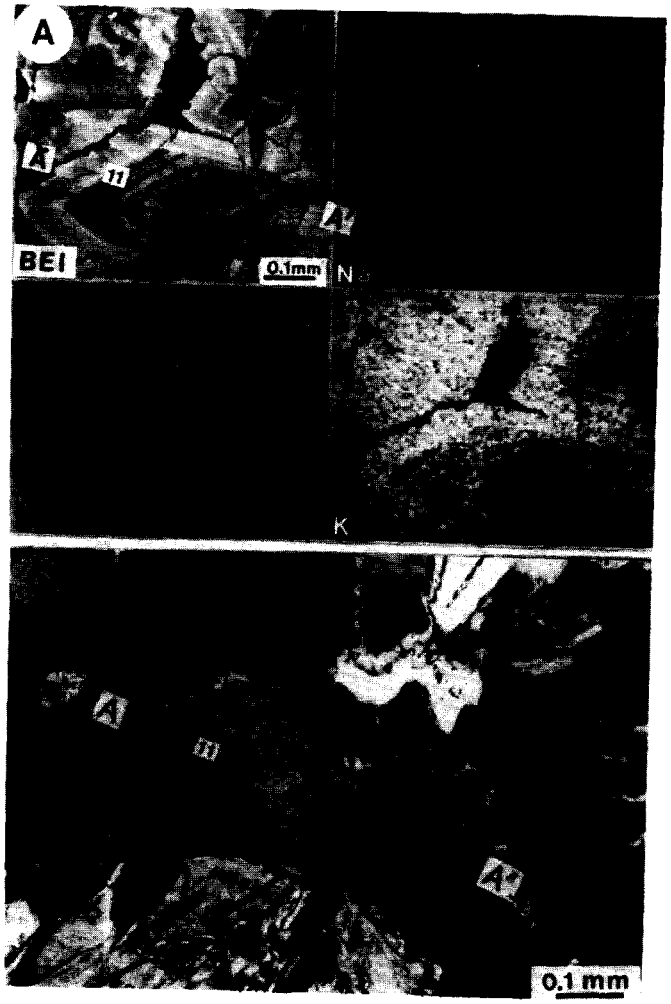

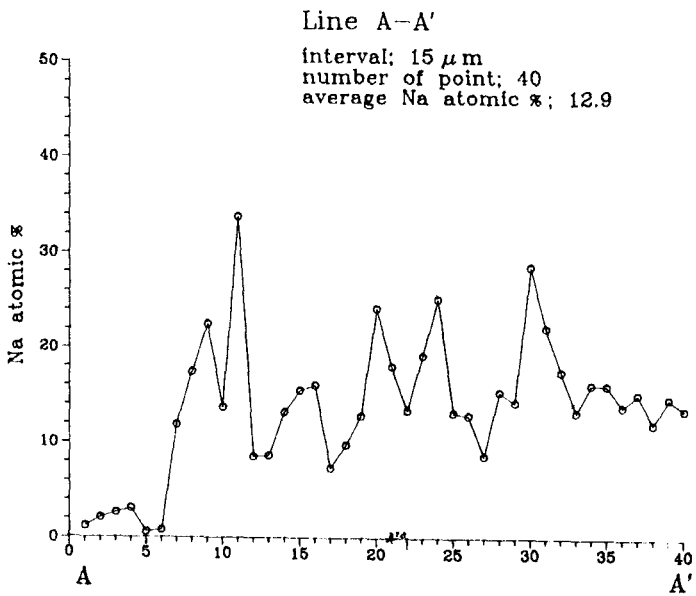

Fig. 3. *Compositional zones in alunite:* (A) Back-scattered electron image (BEI) and X-ray images showing distribution of Na, Si and K (In BEI, 11 indicates analysis point number 11) (B) Microphotograph of alunite with compositional layer (11 indicates analysis point number 11, crossed nicols); (C) Na atomic % along line A-A'. Na atomic % changes from 0.6 – 33.0 %.

line in a single grain with a beam diameter of 5 μm (Fig. 3).

Back-scattered electron image (BEI) shows several alternate white and black bands. It matches well with the distribution of K.

Distribution of K is constrative with that of Na. Na-rich portion and K-rick portion are uncompatible, i.e., Na-rich portion is poor in K and Na-poor portion is rich in K and, vice versa. That indicates Na^+ can substitute for K^+ in the A site.

Na-rich portion developes along the growth layers of alunite. Distribution of Na in a single grain is uniform in the inner part, considerably flucuates in the middle part, and very low in the outer part. That reflects Na content of solution is changed with the growth of alunite. Na content of solution is nearly uniform at the initial stage of crystallization of alunite in a veinlet, considerably variable at the middle stage, and very low at the last stage. Quantitative analyses present that Na-poor portion contains 20-50 atomic percentage of Na and Na-poor portion 0-10 percentage

XRD analyses were performed for alunite which has different atomic percentage of Na. Quartz was used as an internal standard. XRD patterns were obtained in the region of 10 to 50° (2θ) at a scan speed of 1°(2θ)/min., and repeated 4-6 times for accuracy. Observed data were averaged, indexed after those of Parker (1962), and refined using the least squares program (Appleman and Evans, 1973; Garvey, 1986).

Atomic percentages of Na and unit-cell dimensions of alunite are listed in Table 2. Na atomic percentages of alunite from this mine fluctuates slightly, so that unit-cell dimensions vary in a narrow range.

The c dimension decreases with increasing atomic percentages of Na, but the a dimension shows no certain relationship. However, the unit-cell volume of alunite shows a reverse relationship with atomic percentage of Na in the A site (Fig. 4).

Table 2. Na atomic percentages and unit-cell dimensions of alunite from the Sungsan mine.

#	Na atomic %	a(Å)	c(Å)	c/a	V(Å^3)
A7	9.2	6.978	17.295	2.479	729.3
A8	8.7	6.982	17.279	2.475	729.5
F4	6.6	6.979	17.301	2.480	729.7
C3	6.4	6.981	17.300	2.478	730.1
C1	5.9	6.980	17.320	2.481	730.8
Parker (1962)	3.0	6.981	17.340	2.484	731.8

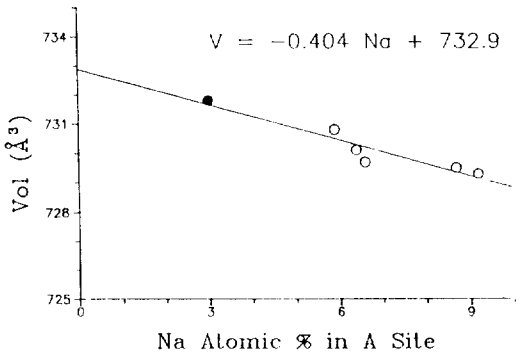

Fig. 4. Unit-cell volume vs. Na atomic percentage in the A site of alunite from the Sungsan mine. Solid circle is from Parker (1962), and open circle from this work.

THERMAL BEHAVIORS

DTA curve of an alunite has two large endothermic peaks and one small exothermic peak. TG and DTG curves show that alunite undergoes two steps of weight loss at different temperature regions (Fig. 5). In order to interpret these curves, XRD analyses were made for the sample heated from 25°C to 1000°C at a rate of 10°C per minute (Fig. 6). At every different temperature, samples were heated for 1 hour.

XRD peaks of alunite decrease in their intensity with increasing temperature, resulting in only a few weak peaks at 550°C. At 575°C, alunite phase disappears completely and one new phase, anhydrous potassium alum, $KAl(SO_4)_2$ appears at 3.68Å. On heating up to 700°C, peaks of anhydrous potassium alum gradually become strong, and those of anhydrous sodium alum, $NaAl(SO_4)_2$ newly appear. At 720°C, peaks of anhydrous alums disappear, whereas those of $Al_2(SO_4)_3$, arcanite (K_2SO_4), thenar-

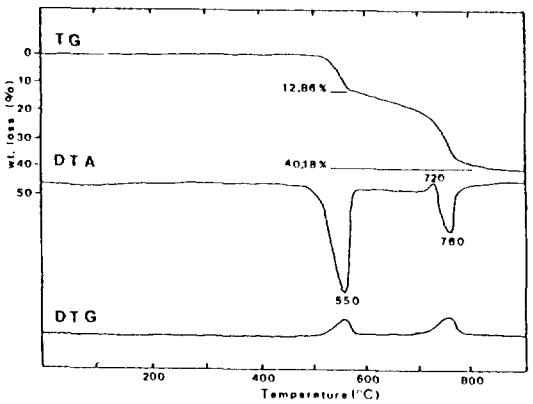

Fig. 5. DTA, TG, and DTG curves of alunite from the Sungsan mine (Heating rate: 10°C/min).

dite(Na_2SO_4) and γ-Al_2O_3 appear. At 760°C, $Al_2(SO_4)_3$ peaks disappear, and with increasing temperature up to 1000°C, arcanite peaks become intense and thenardite and γ-Al_2O_3 peaks weaker. Above 900°C corundum (α-Al_2O_3) peaks appear.

On the basis of the XRD analyses of heat-treated alunite, the thermal curves have been interpreted. The first endothermic peak at 550°C corresponds to the decomposition of alunite into anhydrous K- and Na-alum, with concomittant removal of structural water (12.86%). An exothermic peak at 720°C is ascribed to the decomposition of anhydrous K- and Na-alum into $Al_2(SO_4)_2$, arcanite, thenardite and γ-Al_2O_3. The second endothermic reaction at 760°C represents the destruction of $Al_2(SO_4)_3$ with degassing of 3/4 of total SO_3 (27.32%). K_2SO_4 and Na_2SO_4 phases are stable up to above 1000°C whereas γ-Al_2O_3 converts to α-Al_2O_3 above 900°C.

Kashkai and Babaev (1969) suggested that the multiplication of the amount of SO_3 indicated by the second endothermic peak by 4/3 gives total SO_3 and that the area of the peak be used as a measure of the percentage of alunite in alunitized rocks. In this study, total SO_3 content computed after Kashkai and Babaev's method is 36.43 wt. %, and that the analyzed value by EPMA is 38.64 wt. %. This indicates that the Kashkai and Babaev's method is apparently reasonable.

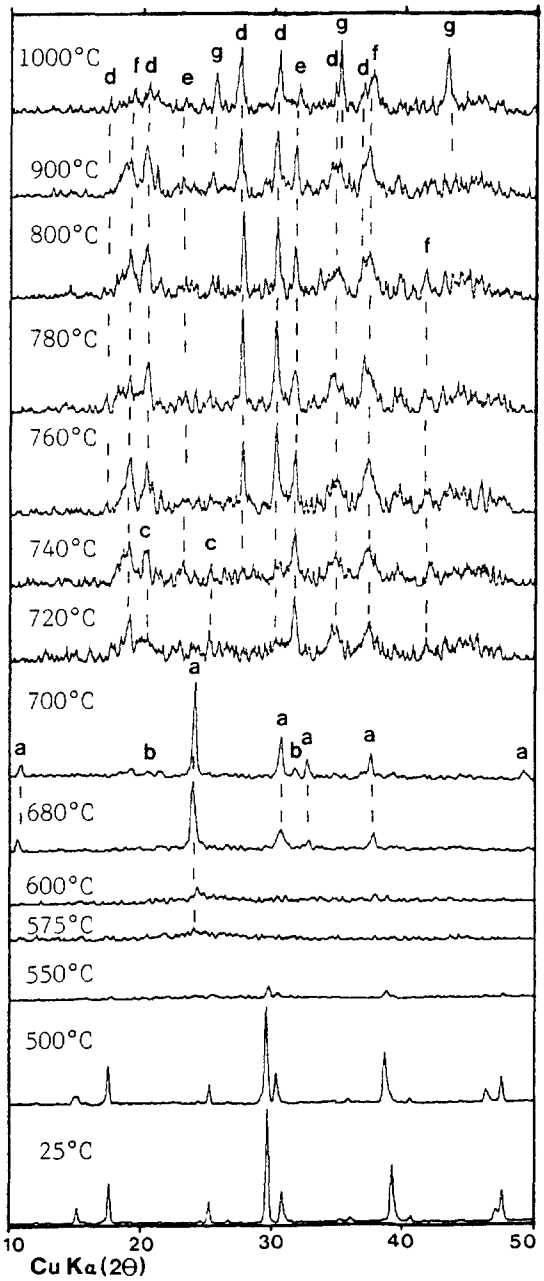

Fig. 6. XRD patterns of heat-treated samples of alunite from 25°C to 1000°C: a: $KAl(SO_4)_2$, b: $NaAl(SO_4)_2$, c; $Al_2(SO_4)_3$, d; K_2SO_4 (arcanite), e; Na_2SO_4 (thenardite), f; γ-Al_2O_3, g; α-Al_2O_3 (corundum).

IR ABSORPTION SPECTROSCOPY

IR absorption spectrum of an alunite from the Sungsan mine (Fig. 7) is similar to those from Marysvale, Utah (van der Marel and Beutelspacher, 1976). Absortion bands due to the sulphate ions on C_{3v} sites are assigned to ν_1 at 1025cm^{-1}, ν_2 at 465cm^{-1}, ν_3 at 1080 and 1220cm^{-1}, and ν_4 at 588 and 616cm^{-1}. The first one is A_1 (symmetric stretching vibration), the second one, E (bending vibration), and the other two, A_1+E modes. IR bands at 3487cm^{-1} is interpreted as OH-stretching vibration (Adler and Kerr, 1965; Ross, 1974).

By Brophy and Sheridan (1965) and Kubisz (1972), a deficiency in the A site coupled with an analytical excess of water has generally been interpreted as due to the replacement of A^+ ions by H_3O^+ on the basis of the alunite solid solution studies. H_3O^+ ion has distingushable ν_4 vibration (E mode) in the region 1500-1700cm^{-1}. Thus the possibility of the presence of H_3O^+ ion may be detectable from IR spectrum (Wilkins and Mateen, 1974). But an alunite from the Sungsan mine (A7) has neither alkali ion deficiency nor excess water. Moreover it has not IR bands in the 1500-1700cm^{-1} range. We suggest that H_3O^+ ion is not present in the alunite from this mine. But other alunite samples such as F4 or A8 have alkali ion deficiencies, need to be further studied whether or not H_3O^+ ions are present in the A site.

Acknowledgments: This research was supported by the grant given to the first author (H.G. Cho) from the Daewoo Foundation. We thank Mr. H.S. Choi for his kind assistance in the electron microprobe analyses and SEM photographs, and Mr. J.N. Park for the use of thermal analyzer.

REFERENCES

Alder, H.H. and Kerr, P.F. (1965) Variations in infrared spectra, molecular symmetry and site symmetry of sulfate minerals. Amer. Miner., 50, 132-147.

Appleman, D.E. and Evans, H.T. (1973) Job 9214: Indexing and least-squares refinement of powder diffraction data. U.S. Geol. Surv. Publ. Compu. Contrib., 20, U.S. Nat. Tech. Inf. Service, Doc. PB2-16188.

Brophy, G.P., Scott, E. S., and Snellgrove, R.A. (1962) Sulfate studies. II: Solid solution between alunite and jarosite. Amer. Miner., 47, 112-126.

Brophy, G.P. and Sheridan, M.F. (1965) Sulphate studies. IV: The jarosite-natrojarosite-hydronium jarosite solid solution series. Amer. Miner., 50, 1595-1607.

Chitale, D.V. and Güven, N. (1987) Natroalunite in a laterite profile over Deccan trap basalts at Matanumad, Kutch, India. Clays Clay Miner., 35, 196-202.

Garvey, R. (1986) Computer Program "LSUCRIPC" (Least Squares Unit Cell Refinement with Indexing on the Personal Computer). Powder Diffraction, 1, 114.

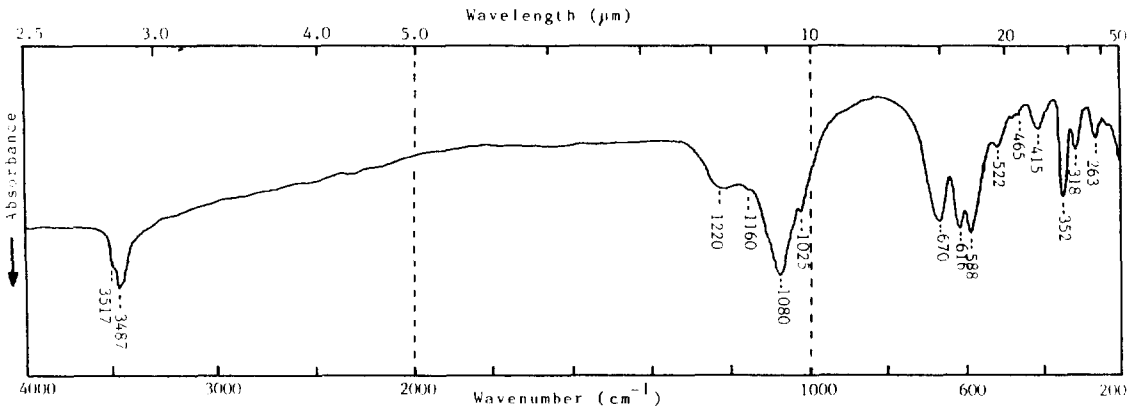

Fig. 7. Infrared absorption spectrum of alunite from the Sungsan mine.

Goreaud, M. and Raveau, B. (1980) Alunite and crandallite: A structure derived from that of pyrochlore. Amer. Miner., 65, 953-956.

Hendricks, S.B. (1937) The crystal structure of alunite and the jarosites. Amer. Miner., 22, 773-784.

Kashkai, M.A. and Babaev, I.A. (1969) Thermal investigations of alunite and its mixtures with quartz and dickite. Miner. Mag., 37, 128-134.

Kubisz, J. (1970) Studies on synthetic alkali-hydronium jarosites. I: Synthesis of jarosite and natrojarosite. Mineralogia Polonica, 1, 47-58.

Kubisz, J. (1972) Studies on synthetic alkali-hydronium jarosites. III: Infrared absorption study. Mineraloia Polonica, 3, 23-37.

Menchetti, S. and Sabelli, C. (1976) Crystal chemistry of the alunite series: Crystal structure refinement of alunite and synthetic jarosite. Neues Jahrbuch für Miner. Monat., 9, 406-417.

Moon, H.S. (1975) A study on genesis of alunite deposits of Jeonnam area. Jour. Korean Inst. Mining Geol., 8, 183-202 (in Korean).

Osska, J.O., Hirabayashi, J.-I., Okada, K., Kobayashi, R., and Hayashi, T. (1982) Crystal structure of minamiite, a new mineral of alunite group. Amer. Miner., 67, 114-119.

Parker, R.L. (1962) Isomorphous substitution in natural and synthetic alunite. Amer. Miner., 47, 127-136.

Ripmeester, J.A., Patcliffe, C.I., Dutrizac, J.E., and Jambor, J.L. (1986) Hydronium in the alunite-jarosite group. Canad. Miner., 24, 435-447.

Ross, S.D. (1974) Sulphates and other oxy-anions of group VI. In: V.C. Farmer (ed.) The Infrared Spectra of Minerals. Miner. Soc. Monograph 4, 423-444.

Sang, K.N. (1986) Some aspects of kaoline-pyrophyllite deposits in Southern Korea. Jour. Korean Inst. Mining Geol., 19, Spec. Iss., 43-52 (in Korean).

Scott, K.M. (1987) Solid solution in, and classification of, gossan-derived members of the alunite-jarosite family, northwest Queensland, Australia. Amer. Miner., 72, 178-187.

Stephen, P. A., Fitzpatrick, J.J., Krohn, M.D., Bethke, P.M., Hayba, D.O., Goss, J.A., and Brown, Z.A. (1988) Ammonium in alunites. Amer. Miner., 73, 145-152.

Van der Marel, H.W. and Beutelspacher, H. (1976) Atlas of Infrared Spectroscopy of Clay Minerals and their Admixtures. Elsevier, Amsterdam, 340-345.

Wang, R., Bradley, W.F., and Steinfink, H. (1965) The crystal structure of alunite. Acta Cryst., 18, 249-252.

Wilkins, R.W.T. and Mateen, A. (1974) The spectroscopic study of oxonium ions in minerals. Amer. Miner., 59, 811-819.